# Developing thermoplastic hybrid titanium composite laminates (HTCLS) at room temperature: Low-velocity impact analyses

M.E. Kazemi[1,2], M. Bodaghi[3], L. Shanmugam[2], M. Fotouhi[4], L. Yang[5], W. Zhang[1*], J. Yang[2*]

[1]Department of Mechanical and Automation Engineering, The Chinese University of Hong Kong, Shatin, NT, Hong Kong SAR

[2]Department of Mechanical and Aerospace Engineering, The Hong Kong University of Science and Technology, Clear Water Bay, Kowloon, Hong Kong SAR

[3]Department of Engineering, School of Science and Technology, Nottingham Trent University, Nottingham NG11 8NS, United Kingdom

[4]School of Engineering, University of Glasgow, Glasgow G12 8QQ, United Kingdom

[5]College of Civil and Transportation Engineering, Shenzhen University, Shenzhen, China

[*]Corresponding authors. Emails: maeyang@ust.hk; weizhaozhang@cuhk.edu.hk

## Abstract

Hybrid titanium composite laminates (HTCLs) are high-performance light-weight fiber metal laminates (FMLs) that are being increasingly used in various industries such as aeronautical, military, and marine thanks to their optimized fracture toughness, impact resistance, and thermal performance. In the current study, the low-velocity impact (LVI) characteristics of a new generation of thermoplastic (TP) HTCLs at various energy levels are investigated. To do so, Ti-6Al-4V sheets, carbon fabrics, and ultra-high molecular weight polyethylene (UHMWPE) fabrics are used to fabricate multiple laminates with different fiber types, metal volume fractions, and lamination layups. A low-cost resin infusion process is employed for manufacturing the laminates at room temperature by using a novel liquid

thermoplastic methyl methacrylate resin, Elium® 188. Before fabrication, a multi-step surface treatment method is applied on Ti alloy sheets to enhance the interfacial properties between the composite layer and the metal alloy sheet. In addition to TP-HTCLs, equivalent thermosetting (TS) HTCLs with an epoxy resin, Epolam, are fabricated to compare the results and evaluate the possibility of fabricating recyclable TP-FMLs at room temperature with enhanced out-of-plane properties. Impact properties including contact force, deflection, energy parameters, and related damage modes are investigated and presented for each laminate. It is concluded that the newly developed TP-HTCLs can be cured at room temperature and have enhanced impact properties compared to those of TS-HTCLs. Besides, the HTCL with UHMWPE fabrics on its composite sides (before the Ti alloy sheets) performs better in LVI compared to that with carbon fibers on the top and bottom (of its composite core) since UHMWPE exhibits higher strain to failure and fracture toughness compared to carbon fibers.

**Keywords:** Hybrid titanium composite laminate (HTCL), Low-velocity impact; Thermoplastic resin; Fiber-reinforced polymer (FRP)

## 1 Introduction

Fiber metal laminates (FMLs) are hybrid structures combining thin layers of metal alloy sheets and fiber-reinforced polymer composites (FRPCs) [1]. They enjoy the durability, toughness, and impact resistance of metal alloys and the outstanding in-plane mechanical properties offered by FRPCs [2-4]. In fabricating different types of FMLs, various factors such as stiffness, impact performance, density, corrosion, and operating temperatures have driven the motivation of choosing different metal alloy sheets, namely aluminum,

magnesium, titanium, and stainless steel [5-7]. In this regard, aluminum-based FMLs are being widely used in miscellaneous industries such as aerospace, which have received considerable attention in the literature regarding their applications and mechanical characteristics [8, 9]. However, they exhibit some limitations on elevated operating temperatures as well as damage tolerance in harsh environmental conditions [10]. Magnesium alloys thanks to their low density, low cost, and superior corrosive properties compared to aluminum alloys are also being used in manufacturing FMLs, especially in the automotive industry [11, 12]. However, the low stiffness of magnesium alloys requires thick sheets in fabrication; as a result, in terms of specific properties, they do not differ significantly from aluminum alloys. Besides, due to their limitations in high temperatures, magnesium alloys may not be suitable for high-performance impact applications while they offer outstanding properties in compression [13]. Stainless steel alloys are comparable to titanium alloys in terms of stiffness, and applying them eliminates the galvanic corrosion in the aluminum-based FMLs (which contain carbon fibers) [14, 15]; however, their density is higher than that of titanium (Ti) alloys and do not possess excellent corrosive properties of Ti alloys [13]. Ti alloys enjoy outstanding corrosive and mechanical properties, such as superior stiffness, strength, fatigue, impact performance, and operating at elevated temperatures [16].

Concerning the low-velocity impact (LVI) response of Ti-based FMLs, which are known as hybrid titanium composite laminates (HTCL), there are limited studies in the literature, which mainly emphasized the use of carbon or glass fibers mostly with thermosetting (TS) or traditional thermoplastic (TP) resins, such as PEEK [17]. One of the early studies was performed by Bernhardt et al. [18]. They manufactured HTCLs with a 2/1 layup consisting

Ti-15-3-3-3 alloy foils and IM-6 graphite and compared the results in LVI with those of monolithic FRPCs in terms of lamina orientation and stacking sequence. They concluded that HTCLs offer better impact performance compared to that of monolithic composites with a smaller damaged zone. Besides, due to the buckling of the top Ti alloy during the impact event, the inspection and repairing of the laminate would be easier compared to FRPCs. In another study, the LVI behavior of HTCLs made of carbon/PEEK laminates and glass poly-ether-imide (PEI) laminates was studied by Cortes and Cantwell [19]. They demonstrated that glass-based HTCL enjoys higher specific perforation energy than that of carbon-based HTCL. Interfacial and interlaminar delamination were reported as the major mechanisms of energy absorption in LVI. In addition to this study, there have been quite a few studies regarding the LVI performance of glass-based HTCLs conducted by Jakubczak and his team [20, 21]. They compared the behavior of glass-based HTCLs with that of carbon-based FMLs (CARALL) and monolithic CFRP and concluded that HTCLs have higher impact resistance than CARALLs (two times) and than CFRP (six times) in terms of impact energy. As the metal composite interface (MCI) significantly affects the mechanical characteristics of FMLs, specifically in out-of-plane response (such as impact), Li et al. [10] applied three different multi-step surface treatment methods to enhance the interface and compare the LVI performance of HTCLs. In their next study, they investigated responses of two types of HTCLs in high-velocity impact (HVI) regimes [16]. The fabricated laminates were made of plain weave carbon fabrics with epoxy resin (in a VARI process) and ultra-high molecular weight polyethylene (UHMWPE) prepregs in a hot-press procedure. They found out that the ballistic performance of HTCLs containing UHMWPE fibers is greater compared to that of

HTCLs made of carbon fibers. Besides, the rolling direction of the Ti alloy sheet remarkably affects the result in terms of absorbed energy through different failure modes.

Recently, UHMWPE fibers are being replaced by carbon/glass fibers in manufacturing FRPCs and FMLs for impact applications thanks to their outstanding impact performance and low density [22-25]. Although UHMWPE-based FRPCs show good impact resistance in ballistic and HVI applications, the low stiffness of UHMWPE-based laminates does not make them suitable for applications that require high stiffness [26]. A potential solution to overcome such a challenge is hybridizing UHMWPE fibers with stiff metal alloys, such as Ti and aluminum (Al) [27-29], or further hybridizing them with high stiffness fibers such as carbon fibers [30]. To the best of the authors' knowledge, there has been no study on the LVI response of laminates made of hybrid FRPC laminates (comprising UHMWPE and carbon fabrics) and Ti alloy sheets. Besides, most of the previous studies fabricated and investigated HTCLs with TS resins, which exhibit brittle behavior in the LVI response. In some limited studies, researchers used conventional TP resins, namely CBT, PEEK, and PU, which need high temperature and expensive equipment for processing. As a consequence, using those resins results in higher costs and labor works, and moreover, causes thermal residual stresses induced during manufacturing. Those traditional TP resins also cannot be processed in the vacuum-assisted resin infusion (VARI) process [30, 31]. To overcome those problems, a novel liquid thermoplastic methyl methacrylate resin, Elium® 188, is used for fabricating the HTCLs at room temperature with the VARI process [28, 32-34]. The first significant novelty of the current research work is introducing new recyclable TP-HTCLs for LVI applications manufactured for the first time at room temperature, with the possibility of improving impact performance and reducing production time and cost (compared to their traditional TP and TS

counterparts). Second, different hybrid systems are introduced to propose new systems with trade-off mechanical properties (in terms of stiffness and impact performance) compared to HTCLs with a single type of fiber-reinforcements. Third, a new complete thermoplastic system (comprising a TP resin, UHMWPE fibers, and Ti alloys) is introduced, which can be a promising option for LVI applications. In this regard, HTCLs are fabricated in 2/1 layups with carbon fabrics, UHMWPE fabrics, and their hybrid composite systems. Prior to fabrication, a recently developed multi-step surface treatment is applied to improve the interfacial properties between the composite core and the metal alloy sheet [10]. Besides, Epolam epoxy resin is used to fabricate equivalent TS-HTCL to further compare the results. LVI properties, such as maximum contact force, displacement, energy characteristics, as well as damage modes for different TP-HTCLs are investigated and compared for each laminate.

## 2 Materials and Methods

Thermoplastic hybrid titanium composite laminates (TP-HTCLs) investigated in the present study have 2/1 layups made of Ti-6Al-4V sheets with the thickness of 0.4 mm provided from BaoJi Chuang Xin Metal Materials, plain weave carbon fabrics (Hexforce-282) with the areal density of 197 g/m$^2$, and plain weave ultra-high molecular weight polyethylene (UHMWPE) fabrics from Quantaflex with the areal density of 172 g/m$^2$. In addition to UHMWPE-based and carbon-based HTCLs, hybrid composite laminates with different layups containing alternative carbon/UHMWPE fabrics are also used as composite cores in fabricating HTCLs. The geometries of the plain weave fabrics are provided in a previous study [26]. Before fabrication, Ti alloy sheets are surface treated to achieve proper bonding [35]. In this regard, Ti alloy sheets are cleaned with sandpaper with a grit size of 400 and then sandblasted by

pressured alumina powder with a particle diameter of 5–200 μm. Sandblasting procedure removes any contamination or undesired oxide layer and also improves the roughness of the surface, see Fig. 1 (a). However, it has been shown that applying only sandblasting does not result in a firm bonding [29]. Thus, in the next step, the Ti sheets were anodized for 15 minutes at 15 V in a 40 ºC anodizing solution consisting 0.1 M of EDTA, 0.2 M of Na-tartrate, and 7.5 M of NaOH. However, applying anodizing treatment results in the dissolve of formed microscopic bumps (that were initially created during sandblasting [36]), see Fig. 1 (b). Thus, the anodized Ti sheets were etched in an etching solution, consisting 1 M of NaOH for 24 hrs at 60 ºC. By applying the etching treatment, nanostructured bumps are formed on the surface of Ti alloy (Fig. 1 (c)). However, that oxide layer is not mechanically stable (since it contains a great amount of water and hydrated ions). Hence, the etched sheets were annealed in a furnace for 5 hours at 600 ºC to stabilize the formed oxide layer and remove residual stresses induced during the sandblasting procedure (Fig. 1 (d)) [36]. After completing the surface treatment, the resin infusion process is followed for far fabricating the HTCLs [26], see Fig. 2 (a). For infusion, a thermoplastic (TP) (liquid methyl methacrylate resin, Elium® 188) is used, which polymerizes with 2 % weight of benzoyl peroxide (BPO) as an initiator to polymerize and forms to PMMA. Also, a two-part epoxy system, Epolam 5015/5015, as an equivalent thermosetting (TS) resin is used for fabrication to compare the effect of resin type on the response of HTCLs in LVI. The thermoplastic HTCLs are fabricated at room temperature, and the thermosetting HTCLs are fabricated at 80 °C for 8 hours. The schematic for some of the HTCLs fabricated in this study is provided in Fig. 2 (b). After curing, the laminates are taken out from the setup and cut by (abrasive) waterjet cutting machine with the sample size of $100\,mm \times 100\,mm$. Different properties of the

HTCLs, namely laminates name, layup, thickness, areal density, and metal volume fraction (MVF) are presented in Table 1. Fig. 2 (c-d) illustrate the cross-sections of HTCL-1E and HTCL-4E as examples, which comprise carbon and UHMWPE fabrics, respectively. Besides, another carbon-based HTCL with a higher value of MVF is fabricated (which has a similar thickness to that of UHMWPE-based HTCL) to compare the effect of MVF and the influence of fiber on the LVI characteristics of HTCLs. In this study, low-energy impact tests are carried out. Based on some preliminary tests, various impact energies from 15 J to 52 J, corresponding to 2.1 m/s to 4.0 m/s, are chosen to observe all the impact scenarios, including rebounding, penetration, and perforation [37, 38]. The total weight of the impactor is 6.61 kg, which has a hemispherical shape with a diameter of 12.7 mm. At each impact test, the force-time curve of the laminate is obtained by a sensor (attached to the impactor) and a data logger system. The impact machine has a pneumatic anti-bounce mechanism to prevent inducing extra damage to specimens after the first impact. The impact machine includes a pneumatic anti-bounce mechanism Then, ASTM D7136 is conducted to obtain the force-deflection curves and energy attributes. In order to analyze the failure modes and compare the rear side of the HTCLs, a high-speed camera is located in the test setup.

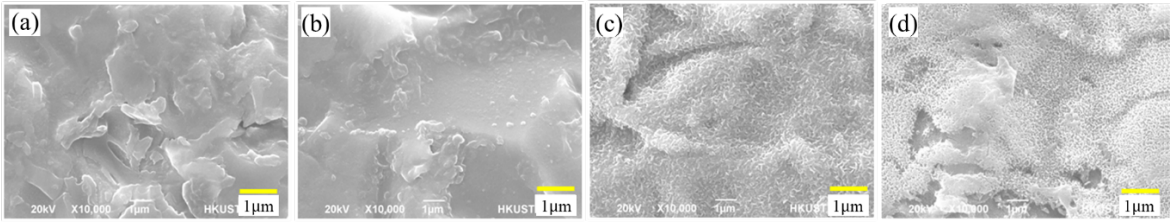


Fig. 1. Scanning electron microscopy (SEM) observations of the surface of titanium (Ti) alloy sheet after sandblasting (a), anodizing (b), etching (c), and annealing (d) surface treatments

Table 1. Laminates name, layup, thickness, areal density, surface treatment, and metal volume fraction of HTCLs

| Laminate Name[1] | Lamination Layup[2] | Laminate thickness (mm) | Areal density ($kg/m^2$) | Surface Treatment[3] | Metal volume fraction |
|---|---|---|---|---|---|
| HTCL-1E | $(Ti/Cf_2)_S$ | 1.70 ±0.05 | 4.83 ± 0.21 | S-Ad-E-An | 0.47 ± 0.02 |
| HTCL-2E | (Ti/Cf/PEf)s | 2.05 ± 0.05 | 5.04 ± 0.27 | S-Ad-E-An | 0.39 ± 0.01 |
| HTCL-3E | (Ti/PEf/Cf)s | 2.10 ± 0.03 | 5.16 ± 0.25 | S-Ad-E-An | 0.38 ± 0.01 |
| HTCL-4E | $(Ti/PEf_3)_S$ | 2.85 ± 0.05 | 5.76 ± 0.31 | S-Ad-E-An | 0.28 ± 0.01 |
| HTCL-5E | $(Ti/Cf_5)_S$ | 2.83 ± 0.05 | 8.09 ± 0.32 | S-Ad-E-An | 0.72 ± 0.03 |
| HTCL-4P | $(Ti/PEf_3)_S$ | 2.85 ± 0.05 | 5.77 ± 0.29 | S-Ad-E-An | 0.29 ± 0.01 |

[1]E: Elium® resin, P: Epolam Resin
[2]Ti: titanium alloy, Cf: Carbon fabric, PEf: UHMWPE fabric
[3]S: Sandblasting, Ad: Anodizing, E: Etching, An: Annealing

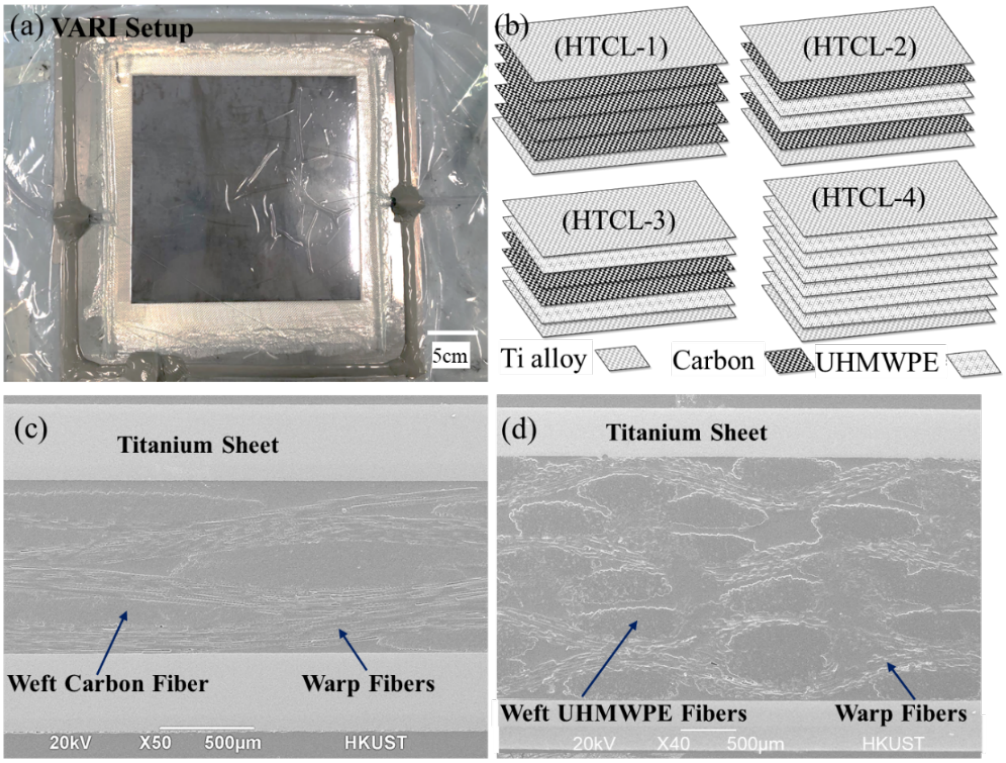


Fig. 2. Vacuum-assisted resin infusion setup (VARI) (a), schematic of lamination layups for different HTCLs (b), warp and weft fibers in sandwiched composites in HTCL-1E (c), and HTCL-4E (d)

# 3 Results and Discussion

## *3.1 LVI characteristics of TP-HTCLs*

Force-time, force-deflection, energy characteristics, and damage/failure modes regarding the low-velocity impact (LVI) response of Elium®-based HTCLs are presented in this section. In this regard, the response of different Elium®-based HTCLs is examined, followed by demonstrating the role of fiber type, resin type, and lamination layup on the LVI behavior. Fig. 3 depicts the force versus time response of TP-HTCLs impacted at various energies. HTCL-1E force-time behavior is presented in Fig. 3 (a). At 15 J, HTCL-1E shows a sinusoidal behavior, and no spike or oscillation in the curve is identified. This exhibits that the laminate is still intact and has not yet undergone any damage. As the impact energy increases to 20 J, after reaching the maximum load in the force-time curve (denoted by $L_m$), the structure cannot sustain more load, resulting in a sudden load drop (about 53 %). Such behavior is regarded as supercritical regime, which demonstrates a significant loss in structural integrity [10]. The sudden drop in loading is due to the loss of contact between the laminate and the impactor. Put another way, when a laminate is impacted in a supercritical regime, some of the bottom layers suffer from severe delamination [1], which results in a sudden drop load. In a supercritical regime, two cases can occur. In the first case, after a load drop, an increase in the load is observed, which is due to the transfer of the load to the bottom intact layers, 20 J in Fig. 3 (a). In the second case, impact energy is much higher than the damage tolerance of the laminate (33 J in Fig. 3 (a)). In this situation, after the sudden drop in the load, the load does not increase again, rather decreases close to zero (due to the friction does not reach exactly to zero), and many oscillations at the end of the curve can be observed.

This demonstrates perforation, in which significant delamination and intra-laminar failure such as fiber breakage/pull-out occur [17, 21].

Fig. 3 (b-c) show the force-time behavior of HTCL-2E and HTCL-3E (which have hybrid FRPC laminates with different stacking sequences) under LVI at impact energies of 15 J, 20 J, 33 J, and 40 J. At 15 J, none of the laminates undergoes any damage; by an increase in the impact energy (to 20 J), HTCL-2E shows a supercritical impact. However, in HTCL-3E, when the load increases, it drops negligibly and increases again, followed by many small oscillations/spikes. In this scenario, the damage is barely visible and matrix-cracks appear in the structure. Such a response is considered a subcritical regime. Such a difference between the supercritical and subcritical regime behavior of the hybrid laminates at the same energy level is related to the stacking sequence of the fabrics. HTCL-3E contains UHMWPE fabrics at the sides of its composite core, which those fibers possess higher failure strain and toughness compared to those of carbon fibers. Thus, the combination of UHMWPE/Ti at the sides makes the laminate more ductile, and therefore, can undergo more plastic deformation. At 33 J and 40 J, HTCL-3E and HTCL-4E undergo supercritical regimes. In the supercritical regime, quite a few damage mechanisms attribute to the structural failure, including but not limited to matrix-cracks, debonding between the metal alloy and the FRPC, debonding between the fiber and matrix, delamination, and fiber breakage and shear-out [17]. The force-time response of HTCL-4E demonstrates that, from 15 J to 33 J, the maximum contact force ($L_m$) increases, which is due to the elastic bending of the structure. Afterward, by increasing the energy, the maximum load does not change remarkably, see Fig. 3 (d).

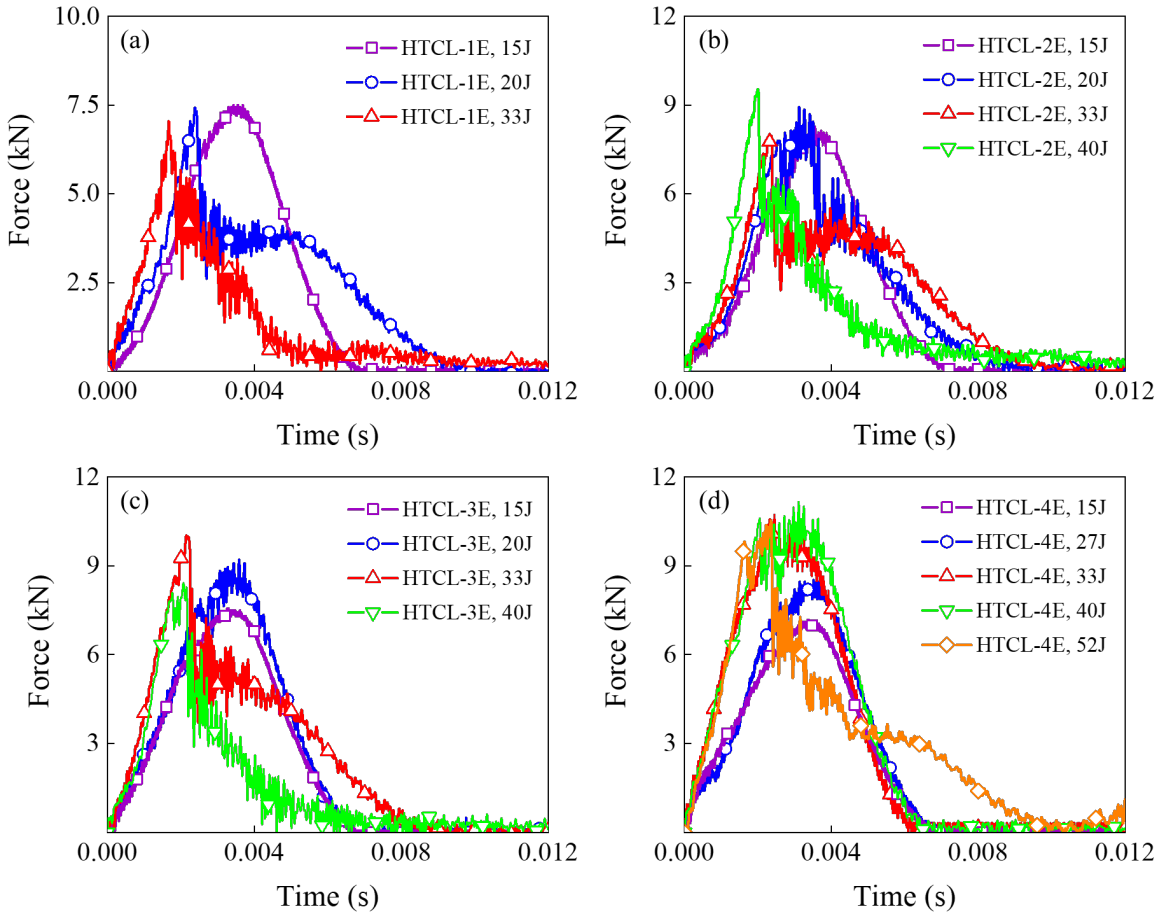


Fig. 3. Contact force versus time curves of (Elium®-based) HTCL-1E (a), HTCL-2E (b), HTCL-3E (c), and HTCL-4E (d) subjected to different LVI tests

The LVI force-deflection response of Elium®-based HTCLs is presented in Fig. 4. Force-deflection curves can provide important information regarding the deflection at maximum load, total deflection (or permanent deflection), and the dynamic modulus of the laminate (slope of the curve). Also, the enclosed area of the curve exhibits the absorbed energy by a laminate in an impact test. During an impact test, three conditions can happen, namely rebound, penetration, and perforation. In rebounding, (15 J in Fig. 4 (a)), after reaching the maximum load, the impactor returns (without a drop in the load-deflection curve). In this case, no damage has happened to the structure [21, 39]. At 20 J, (Fig. 4 (a)), after obtaining the maximum load, the curve shows a drop in the load but increases again till the laminate

reaches its maximum (permanent) deflection. Afterward, the impactor rebounds. At 33 J, after reaching the permanent deflection, the impactor does not return; instead, it goes through all the layers and penetrates the structure. Fig. 4 (b-c) illustrate the force-deflection of the hybrid HTCLs impacted at various impact energies. As can be observed, from 15 J to 40 J, the slope of the curves (laminates' dynamic modulus) increases, since the laminates behave stiffer. Images in Fig. 4 show that by increasing the energy in a specific laminate, the deflection at the maximum load decreases; however, the maximum deflection increases, which shows greater damage to the structural integrity. To show this, the response of HTCL-3E at 15 J and 20 J (Fig. 4 (c)) confirms that there is no difference between the deflection at the maximum load and the maximum deflection; this demonstrates that the laminate is undamaged (except some matrix cracks at most). However, by increasing the energy level, such difference increases. By comparing the difference between the permanent deflection of HTCL-2E and HTCL-3E at 33 J, it is clear that HTCL-2E undergoes more damage and structural integrity loss compared to those presented by HTCL-3E. The force-deflection behavior of HTCL-4E is illustrated in Fig. 4 (d). As can be seen, at all the impact energy levels, rebounding occurs. From 15 J to 33 J, the laminate does not show a remarkable difference between the deflection at the maximum loads and the maximum deflections. Thus, the laminate is considered undamaged. Nonetheless, high transverse shear stresses induce some matrix-cracks near the top layer of the laminate. Nonetheless, going up from 40 J to 52 J, the laminate undergoes a higher degree of damage/delamination.

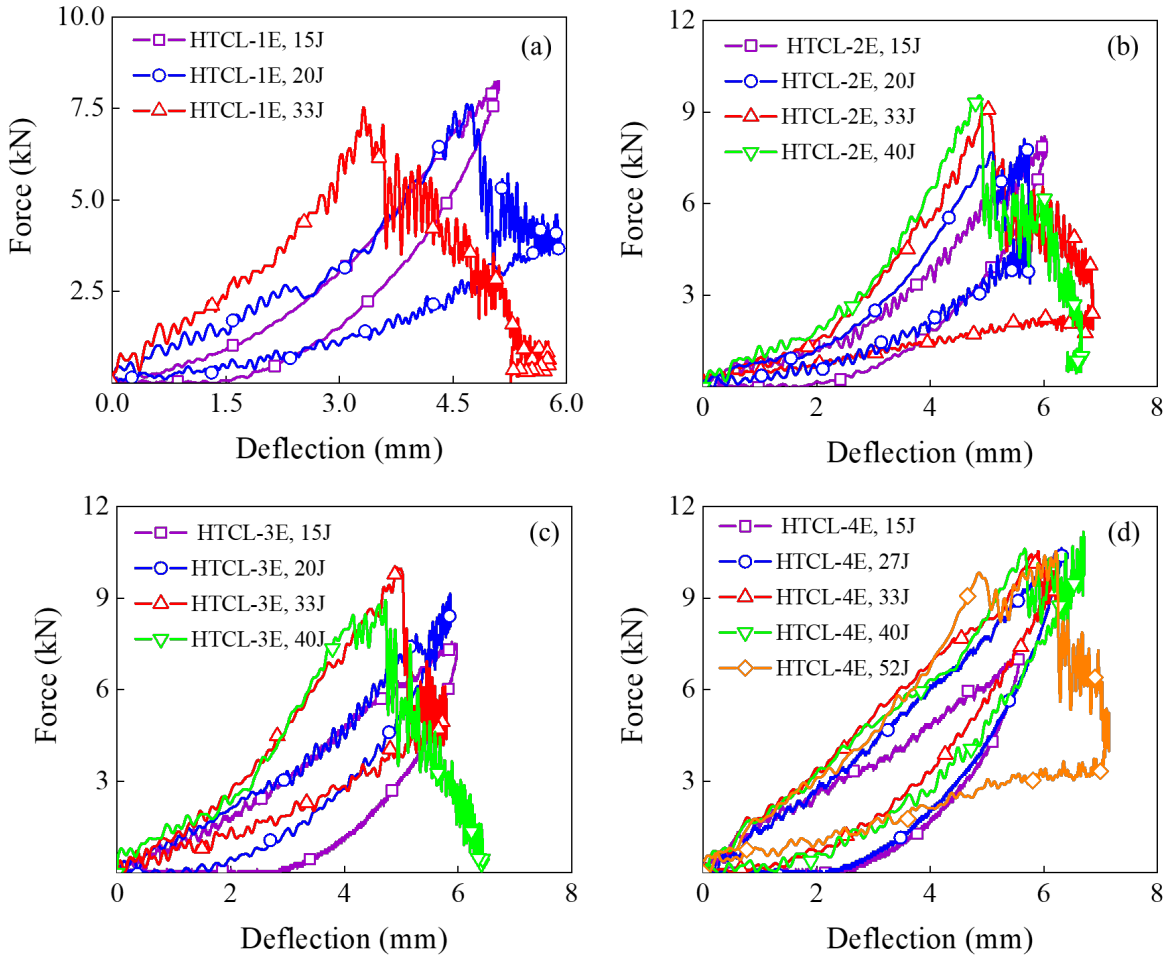


Fig. 4. Contact force versus deflection curves of (Elium®-based) HTCL-1E (a), HTCL-2E (b), HTCL-3E (c), and HTCL-4E (d) subjected to different LVI tests

Fig. 5 shows the energy characteristics of TP-HTCLs subjected to LVI at various impact energies. The energy versus time responses for some of the HTCLs are depicted in Fig. 5 (a). In the case of rebounding, the impact energy, which is also known as peak energy ($E_P$) or saturation energy, is lower than the damage tolerance of the laminate. In rebounding, the energy (in the energy-time profile) increases until the maximum value ($E_P$); afterward, it decreases till achieving a constant flat level. This shows that the laminate cannot absorb more energy, and the value at the end of that plateau level is considered as absorbed energy, shown by $E_{ab}$. The absorbed energy by the laminate may result in different damage modes, namely

matrix cracks, debonding (intra-yarn fracture), delamination (inter-yarn fracture), fiber failure, and plastic deformation for thermoplastic (TP) resins or toughened thermosetting (TS) resins. Fig. 5 (a) shows that rebounding has occurred for HTCL-4E at all the energy levels, for HTCL-2E and HTCL-3E at 15 J, 20 J, 33 J, and for HTCL-1E at 15 J and 20 J. The subtraction of absorbed energy from peak energy is called elastic energy, $E_{el}$, which is the energy kept transiently in the structure and returns to the impactor finally. In penetration, the impactor penetrates the laminate and does not rebound, rather it stops. In this case, the energy-time curve increases till attaining the peak energy. Afterward, it gets a uniform trend without increasing or decreasing. An example of the penetration (energy-time curve) has happened for HTCL-3E at 40 J, Fig. 5 (a). In perforation, the energy-time response of a perforated laminate can be divided into three regions. In the first region, the energy-time increases linearly. Then, it enters a non-linear response (second region). Afterward, the response gets a linear behavior and increases with a constant rate. The point (on the curve) that the response changes from a non-linear behavior to a linear one is called perforation energy (or point), shown by $E_{Pr}$. HTCL-1E energy-time curve at 33 J denotes perforation, see Fig. 5 (a).

Fig. 5 (b) illustrates the variation of maximum contact force for different HTCLs impacted at various energy levels. As was mentioned in the force-time analysis section, as the impact energy increases, the maximum contact force increases (if the impact energy has not reached the damage threshold). For example, for HTCL-4E, the load gradually increases; however, due to the brittle behavior and thinner thickness of HTCL-1E, the load does not change significantly, as it has reached its damage threshold. A valuable criterion for investigating the energy attributes of a laminate in a LVI event is known as major damage energy, $E_{bml}$,

which is the energy of the laminate at the maximum load ($L_m$) [40]. To be specific, it is the amount of absorbed energy before the appearance of the primary failure. Thus, higher values (at fixed impact energy) show a lower damage extent in the laminate. Difference values of major damage energy for HTCL-1E to HTCL-4E are presented in Fig. 5 (c). Comparing the values regarding HTCL-2E and HTCL-3E demonstrates that, in low energy levels, there is not much difference; however, at higher impact energy levels, HTCL-3E that has ductile UHMWPE fibers on the sides of its composite core exhibits higher values of major damage energy, confirming less structural damage compared to HTCL-2E. Fig. 5 (d) shows the values of absorbed energy for each laminate impacted at different energy levels. At low impact energy levels such as 15 J, the laminates show almost the same amount of absorbed energy. However, as impact energy increases to 20 J, HTCL-4E shows lower absorbed energy compared to other HTCLs. At 33 J, the difference between the absorbed energy is more obvious. It should be borne in mind that although all the HTCLs have eight layers of composite plies, the thickness for each core composite laminate varies. As a result, specific absorbed energy, which is the ratio of their absorbed energy to their areal density (Table 1) should be used. Nonetheless, by comparing those values, it is confirmed that HTCL-3E demonstrates lower absorbed energy, and as a consequence, a smaller extent of damage is occurred compared to HTCL-2E. As a result, by changing the stacking sequence in hybrid laminates, a great extent of damage can be prevented. At 33 J, HTCL-1E cannot tolerate the impact energy level and perforates. Its perforation energy is calculated as $E_{Pr,HTCL-1E} = 30$ J.

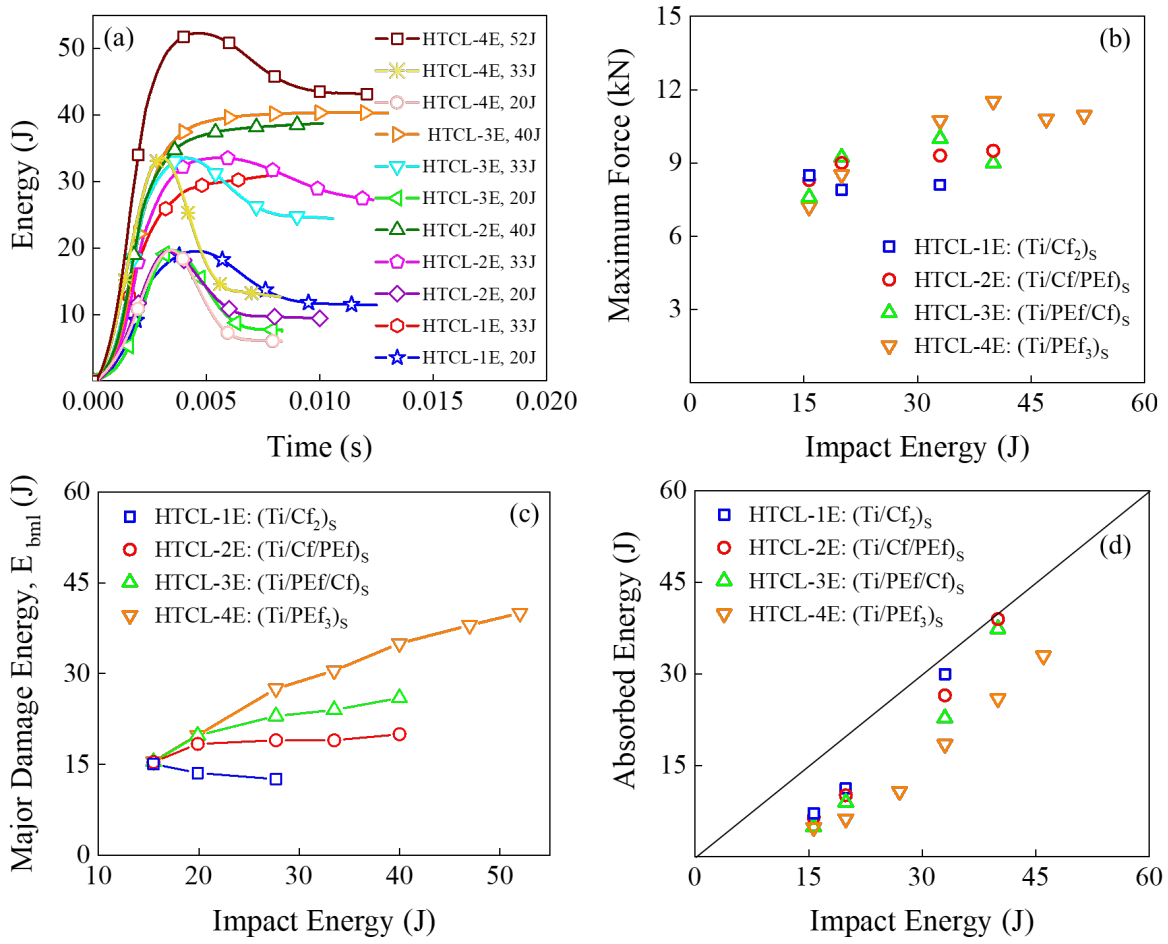


Fig. 5. Energy versus time curves for some of the TP-HTCLs (a), maximum contact force (b), major damage energy values (c), and energy profile diagrams (d) of Elium®-based HTCLs

Non-impacted (rear) and cross-sectional images of HTCLs impacted at 33 J are illustrated in Fig. 6 and Fig. 7, respectively. Those photos provide important information regarding the extent and type of damage in HTCLs. HTCL-1E shows perforation, where the impactor has come out from the other side, Fig. 6 (a). When the impact energy is higher than the damage tolerance of the structure, a long primary crack forms on the rear of the Ti sheet along the rolling direction of the metal [1]. As a result, the rolling direction affects the performance of the FMLs remarkably. When the crack growth reaches a certain value, by increasing the impact energy, the energy is insufficient for the further propagation of the crack (parallel to the rolling direction). Thus, the crack propagates in a direction that has lower crack energy.

The bending of the cracked Ti sheet is also accounted for the change in the direction of the crack, see Fig. 6 (a). Fig. 7 (a) depicts the cross-sectional observations of HTCL-1E. As can be observed, severe debonding has occurred in the interface between the lower Ti alloy and the carbon laminate. This shows that the Ti alloy, thanks to its plastic behavior (compared to brittle carbon fiber) can bend significantly; however, the carbon laminate cannot go under plastic deformation and debonding, delamination, and fiber rupture happen [21]. Fig. 7 (a) demonstrates the breakage of the Ti alloy, which is accompanied by severe carbon fiber fracture in the laminate. However, the damage is local due to the presence of brittle carbon fibers. Fig. 6 (b-c) illustrate the rear side (damaged) Ti sheet of hybrid HTCL-2E and HTCL-3E at 33 J. As can be observed, the formed crack in the rolling direction is longer for HTCL-2E compared to that of HTCL-3E. This is related to the existence of ductile UHMWPE fabrics on the sides of the composite core of HTCL-3E, which lets the composite laminate deforms more, and as a result, absorbs more energy. This precludes the transfer of more tensile load to the rear Ti sheet, and as a result, the growth of the formed crack reduces. Fig. 7 (b-c) demonstrate the cross-sectional images of the HTCLs with hybrid composite cores impacted at 33 J. In this regard, HTCL-3E exhibits less (severe) debonding and delamination. This is thanks to the ductile performance of UHMWPE fibers, which gives more flexibility to the structure. HTCL-2E shows a severe fracture of carbon fibers and UHMWPE fibers. However, a lower extent of damage is seen in (the impacted) HTCL-3E compared to HTCL-2E. Fig. 6 (d) represents the rear side of HTCL-4E at 33 J, which shows a global bulge [4, 10]. The cross-sectional behavior of HTCL-4E also shows that (except some matrix cracking) almost no significant damage has occurred for the laminate, except the plastic deformation of the Ti alloy sheet and the UHMWPE composite in the between.

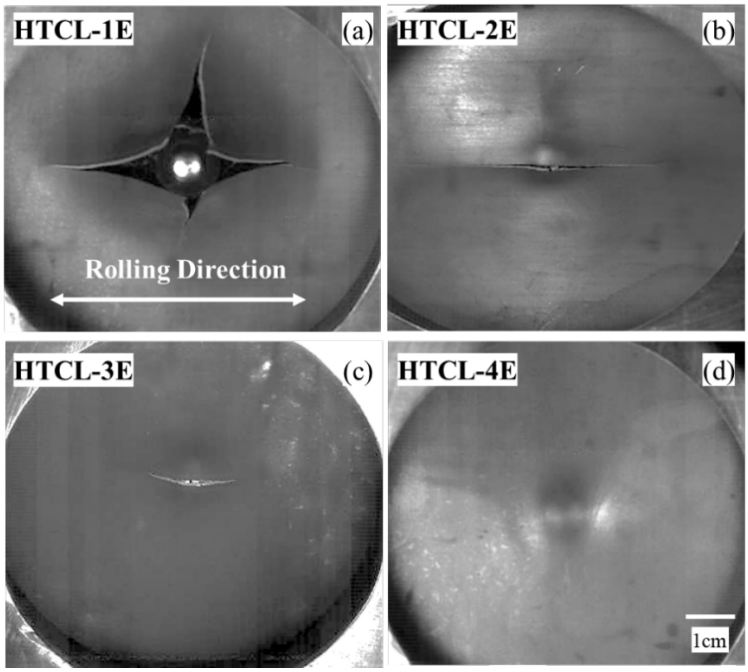


Fig. 6. Final stages of damage on the rear side of HTCL-1E (a), HTCL-2E (b), HTCL-3E (c), and HTCL-4E (d) impacted at 33 J

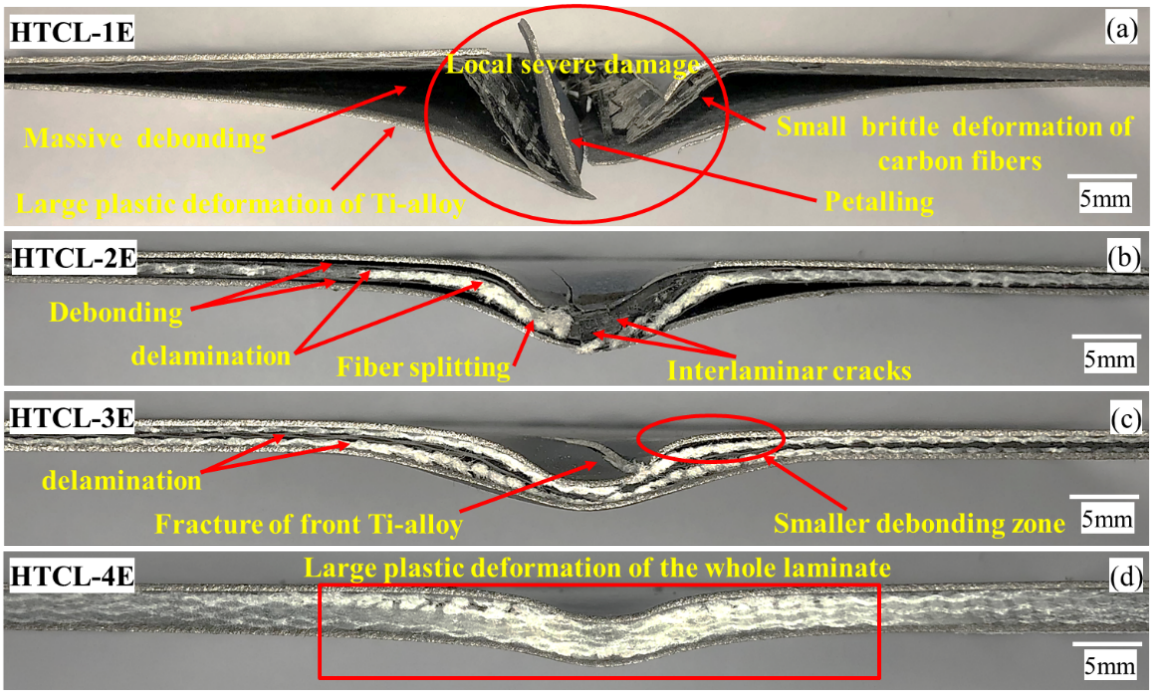


Fig. 7. Macroscopic observations of HTCL-1E (a), HTCL-2E (b), HTCL-3E (c), and HTCL-4E (d) impacted at 33 J

### *3.2 The influence of fiber type and laminates thickness*

To consider the effect of fiber type and metal volume fraction on the LVI response of TP-HTCLs, a thick carbon-based HTCL: HTCL-5E, with the same thickness similar to that of HTCL-4E is fabricated. The force-time, force-deflection, and energy attributes of HTCL-4E versus HTCL-5E are presented in Fig. 8. By comparing the force-time behaviors of the specimens at 33 J and 52 J (Fig. 8 (a)), it is observed that both laminates exhibit almost similar maximum contact forces. However, the time to the load peak is shorter for HTCL-5E compared to that of HTCL-4E, which is due to the brittle response of carbon fibers. Besides, at 33 J, HTCL-4E suffers from a subcritical regime, while the supercritical regime has happened for HTCL-5E. In this regard, the behavior of HTCL-5E at 33 J reveals much more oscillations compared to the behavior of HTCL-4E, which is related to the damage modes that occurred within HTCL-5E, namely matrix-cracking and delamination [1, 41]. By comparing their force-deflection response in Fig. 8 (b), HTCL-5E shows higher dynamic moduli compared to those presented by HTCL-4E at both energy levels. The maximum deflection of HTCL-4E is higher than that of HTCL-5E, showing the ductile behavior of UHMWPE-based HTCLs. Hence, the structural loss in the UHMWPE-based HTCL is much lower compared to that of carbon-based HTCL. To show this, the difference between the deflection at maximum load and the maximum deflection is compared. For HTCL-4E, at both energy levels, such a difference is much lower compared to that in HTCL-5E, Fig. 8 (b). The comparison of energy attributes between HTCL-4E and HTCL-5E is presented in Fig. 8 (c) and Fig. 8 (d). As can be seen in Fig. 8 (c), the absorbed energy between two laminates do not differ significantly at high energy levels. However, by comparing the values

of major damage energy provided in Fig. 8 (d), it is found that HTCL-4E exhibits higher values, demonstrating the lower extent of damage [16].

The rear side and cross-sectional images of HTCL-4E and HTCL-5E impacted at different energies are illustrated in Fig. 9 and Fig. 10, respectively. At 20 J, both laminates present a bulge at the rear side without suffering from supercritical impact. As a result, no crack has been formed on the rear Ti sheets, Fig. 9 (a1-b1). However, the bulge for HTCL-5E (due to the presence of brittle carbon fibers) is local and for HTCL-4E (due to the presence of ductile UHMWPE fibers) is global. Besides, by comparing the cross-sectional images of HTCL-4E and HTCL-5E at 20 J, Fig. 10 (a1-b1), it can be seen that HTCL-5E has undergone a small debonding between the lower Ti sheet and the carbon FRPC laminate in the impact zone, but HTCL-4E is still undamaged, though some matrix cracks (might) have been created within the laminate. Matrix cracks, interlaminar cracks, as well as delamination between the upper plies can be observed as the failure mechanisms in HTCL-5E (at 20 J). However, at this impact energy, matrix cracks and plastic deformation are the only damage modes in HTCL-4E. At 33 J, a crack in the rolling direction forms on the rear side of HTCL-5E (Fig. 9 (a2)), denoting delamination [4]. The corresponding force-time curve, Fig. 8 (a), shows the supercritical impact regime (followed by a significant load drop). Fig. 10 (b2) also confirms this delamination/debonding [4]. In this regard, fibers fracture, interlaminar cracks, matrix cracks, and debonding of the Ti alloy (on both sides) can be observed. However, HTCL-4E still shows no crack (Fig. 9 (b2)), where the corresponding load-time curve demonstrates a subcritical response, and Fig. 10 (b2) shows that debonding has not yet occurred. Fig. 9 (a3-b3) illustrate that at 46 J, a crack forms in the lower Ti sheet of HTCL-4E, and the length of the crack formed previously in HTCL-5E further increases at this energy level. Also, the

cross-sectional images in Fig. 10 (a3-b3) depict that debonding and delamination (which were occurred earlier for HTCL-5E) propagate more, while due to a strong metal composite interface (MCDI), ductile (and tougher) behavior of UHMWPE fibers, debonding does not happen. At 46 J, HTCL-4E exhibits partial delamination within its composite core [17]. At 52 J, the damage mode(s) of UHMWPE-based laminate does not change significantly, while a secondary crack perpendicular to the first one appears in HTCL-5E, (Fig. 9 (a4)). The impact energy level of 52 J demonstrates that, in HTCL-5E, significant delamination has occurred (Fig. 10 (a4)); however, a smaller delamination zone has happened for HTCL-4E [16]. HTCL-4E rear side images show that, as the impact energy increases, the diameter of the bulge, permanent deflections, and the crack length increase (Fig. 9 (b4)). It should be noticed that due to the inert surface of UHMWPE fibers, the interface between the Elium matrix and UHMWPE fibers is intrinsically poor. This is due to the lack of a polar functional group and the low surface free energy of UHMWPE fibers. However, the interface is one of the many parameters affecting the response of the FRP structure in a LVI regime. The ductile nature of Elium® (as a thermoplastic matrix) as well as the tough behavior of UHMWPE fibers contribute to suppressing the crack propagation. To mitigate the interface issue, different fiber surface treatments, namely polydopamine coating [42] can be applied to UHMWPE fibers to improve the interfacial properties between such fibers and the Elium® matrix.

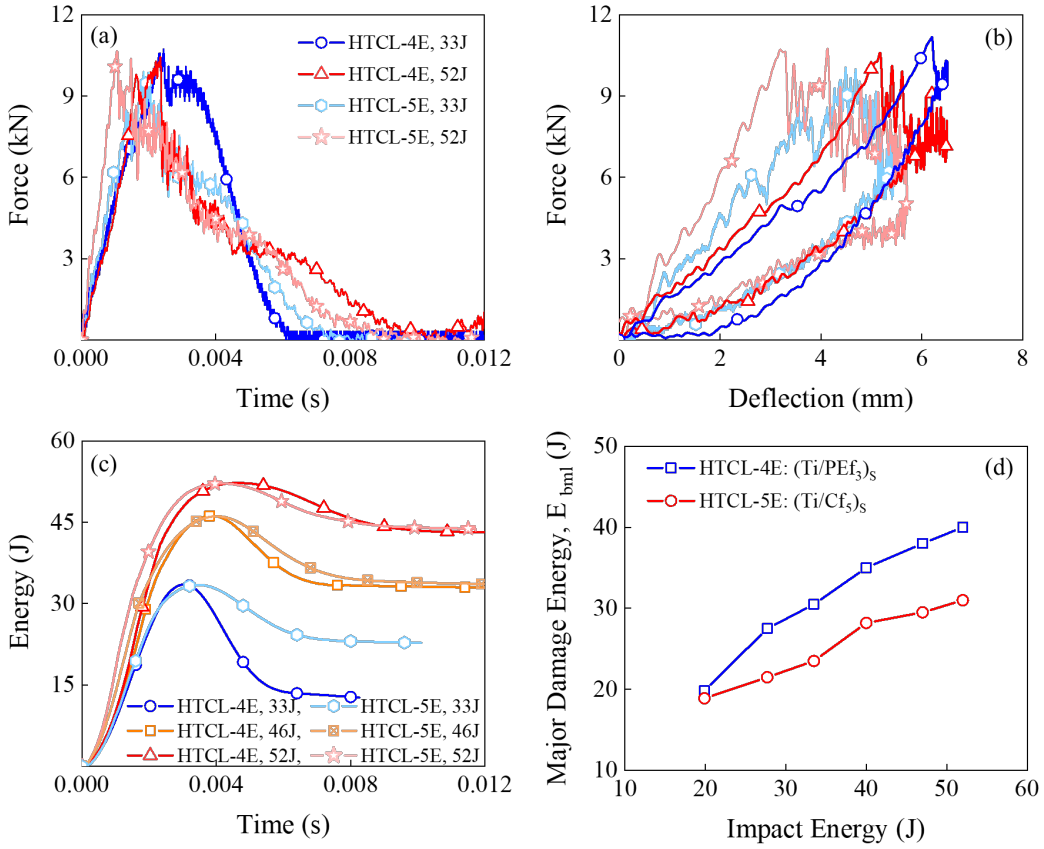


Fig. 8. Force-time (a), force-deflection (b), energy-time (c), and major damage energy (d) attributes of UHMWPE-based and carbon-based HTCLs subjected to different LVI tests

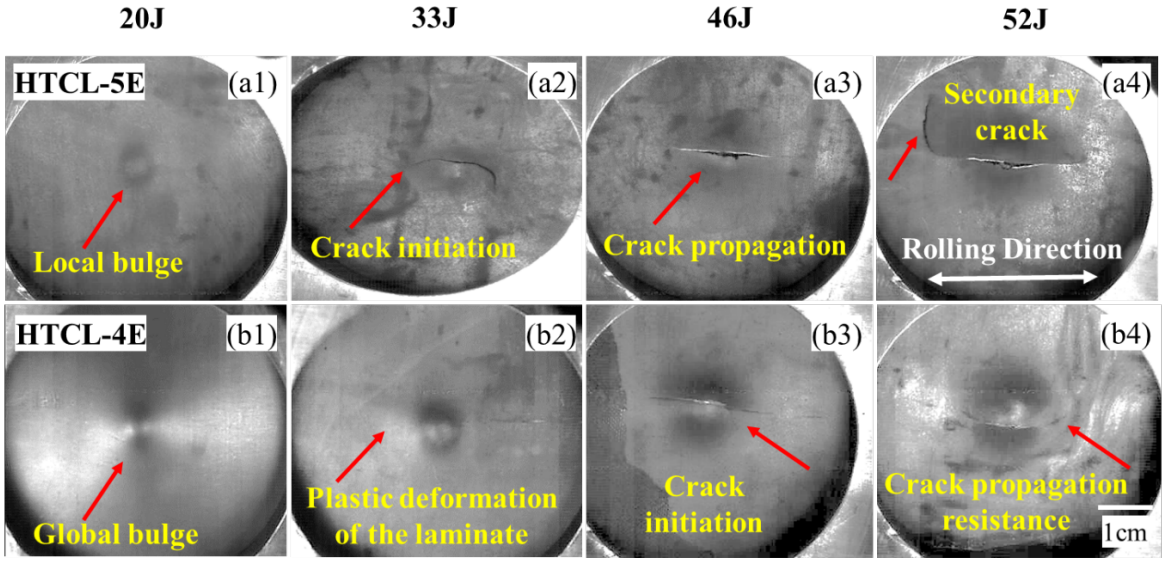


Fig. 9. Final stages of damage on the rear side of HTCL-5E (a1-a4) and HTCL-4E (b1-b4) subjected to different LVI tests

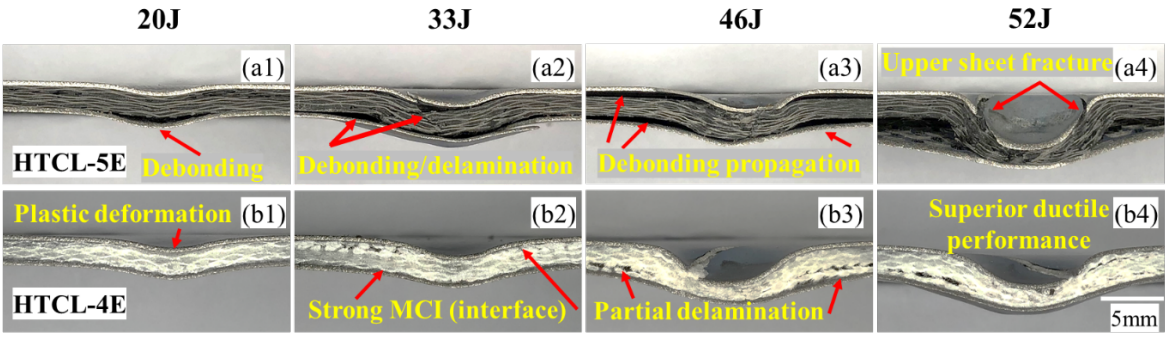


Fig. 10 Macroscopic observations of HTCL-5E (a1-a4) and HTCL-4E (b1-b4) subjected to different LVI tests

As the higher thickness results in a higher impact force, the results can be normalized by a thickness scaling rule to have a fair comparison among the laminates LVI characteristics [43]. Based on this rule, the force-deflection curves for laminates with different thicknesses can be fairly compared, when the forces are scaled up to power 1.5, i.e. $R^{1.5}$, where R is the thickness ratio [44]. As an example, the thickness of HTCL-4E is 2.85 mm and that of HTCL-3E is 2.10 mm. In this regard, the load values of HTCL-4E should be multiplied by the scaling factor of 0.63 $(= (2.1/2.85)^{1.5})$ to have a fair comparison between the contact force of the hybrid system (HTCL-3E) and the fully thermoplastic system (HTCL-4E). As can be observed from Fig. 4, at 40 J, the maximum contact force for HTCL-4E is (about 11.5 kN, which is) higher by 28 % than that of HTCL-3E (which is 9.0 kN). This results in a scaled impact load of 7.25 kN for HTCL-4E (with a thickness of 2.1 mm), which is lower than the maximum contact force of HTCL-3E. This also confirms that, due to the presence of carbon fibers in HTCL-3E, the contact load would be higher compared to that of HTCL-4E. This method can be used and applied for different laminates investigated in this study. However, it should be borne in mind that the thickness scaling approach is a simplified approach to

make the results comparable, and is only valid for the linear part (before the occurrence of delamination) [43].

In order to have a better understanding of damage initiation and propagation in various laminates investigated in this study and also to demonstrate how the position/presence of UHMWPE fabric is playing a major role in deflecting and deviating the crack/damage initiation and propagation, the schematics of overall impact-induced damage pattern in HTCLs (at 33 J as examples) are provided in Fig. 11. Fig. 11 (a) provides an overall schematic regarding some of the common damage modes that happen in a FML under LVI loading. It should be borne in mind that, theoretically, the damage pattern is mirrored from the centerline (i.e. the damage on the left and right sides of the indenter should be roughly the same). However, in reality, due to imperfection during fabrication and testing, this does not usually happen. Moreover, the damage in the Ti alloy sheets, such as bent, tear, and shear are not illustrated and the focus here is mainly on the damage modes in the FRP composite layers in the between. In addition, the schematics provided in Fig. 11 (a-e) are representative of the overall damage pattern and they do not represent the detailed complex damage pattern. Fig. 11 (b-e) demonstrate the impact-induced damage patterns for HTCL-2E to HTCL-5E under LVI loading, which has reverse pine-tree patterns [45]. Due to bending stresses, matrix cracking starts in the lowest layer, and intra-ply cracks and interface delaminations propagate from the lowest surface up toward the impacted surface, see Fig. 11 (b-e). As can be observed in Fig. 11 (c), due to the presence of tough UHMWPE fabrics (in HTCL-3E) near the Ti alloy sheet, the matrix cracking and associated delamination are delayed significantly compared with HTCL-2E, illustrated in Fig. 11 (b), which contains carbon fabrics on the sides. In addition, due to the presence of brittle carbon fabric on the bottom and top of HTCL-3E,

debonding between the Ti layer and carbon fabric happens, as carbon fibers cannot undergo large deformation (Fig. 11 (b, e)). Similarly, the presence of tough UHMWPE fibers in HTCL-4E (Fig. 11 (d)) compared to brittle carbon fibers in HTCL-5E (Fig. 11 (e)) is the main reason for the delayed matrix cracks, resulting in lower delamination/damaged area. Finally, as UHMWPE fibers can undergo a large amount of deformation, the debonding area between UHMWPE fabric and the Ti sheet is significantly smaller compared to that of HTCL-5E, which also confirms acceptable interfacial properties obtained by applying the surface treatment explained earlier.

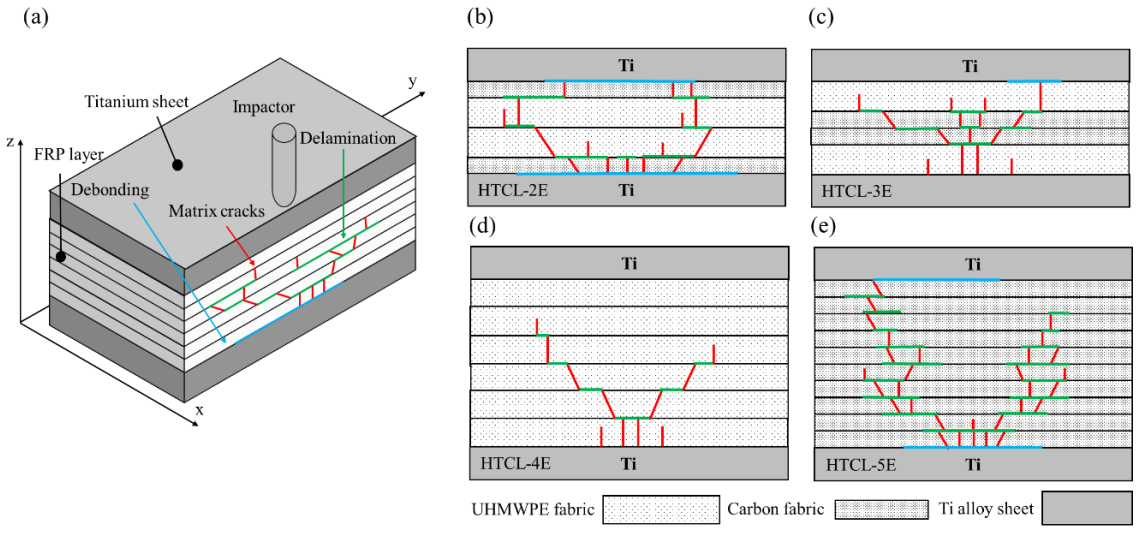


Fig. 11. Schematics of overall impact-induced damage pattern in a FML (a) and in the HTCLs (namely HTCL-2E (b), HTCL-3E (c), HTCL-4E (d), and HTCL-5E (e)) impacted at 33 J

### *3.3 Resin type influence*

This section compares the LVI response for one of the TP-HTCLs developed in this study with a thermosetting (TS)-HTCL counterpart to evaluate the possibility of replacing the TS resins (such as epoxy) in manufacturing FMLs in general and HTCLs in particular with Elium®. The results are provided in Fig. 12, Fig. 13, and Table 2. In this regard, Fig. 12 (a-d) illustrate the force-time, force-deflection, and energy characteristics of UHMWPE-based HTCLs with TP (Elium®) and TS (Epolam) resins. To have a fair comparison, HTCL-4E and HTCL-4P are tested at the same energies. The force-time response is very similar in terms of maximum load and the impact regime in selected energy levels, Fig. 12 (a). However, by analyzing the force-deflection behaviors, it is found that, at 46 J, the dynamic modulus of the HTCL-4P is slightly greater than that of the HTCL-4E. Besides, the maximum deflection of HTCL-4E is higher than that of HTCL-4P, because of the ductile behavior of Elium® resin. By changing the impact energy from 46 J to 52 J, the difference between the maximum deflections remains noticeable. Fig. 12 (c-d) exhibits the energy characteristics of the laminates. At both energies of 33 J and 46 J, the TP laminate absorbs a lower amount of energy. However, by comparing the values of major damage energy, it is noticed that, at low energy levels (20 J to 33 J), HTCL-4E and HTCL-5E absorb the same amount of energy before the major failure happens. However, as the impact energy increases to higher values like 40 J and 46 J, such a difference increases and the TP laminate shows lower values, demonstrating a higher extent of damage in the TS laminate. This demonstrates that in the TP-based structure, before the occurrence of the primary damage, a significant amount of energy is absorbed through plastic-elastic deformations. Fig. 13 also demonstrates that, at 40 J, a crack forms on the rear side Ti sheet in HTCL-4P, which is related to its brittle behavior,

while the rear side Ti sheet in HTCL-4E remains intact. This demonstrates that at 40 J, HTCL-4P should have undergone a supercritical impact regime, while a subcritical regime has occurred for HTCL-4E. At 52 J, the difference increases suddenly. This suggests that the TP laminates show their advantages in high (or critical) impact energy levels. Comparing the results suggests that TP laminates can absorb a higher amount of energy till major damage occurs, which is related to the viscoelastic behavior of the resin, resulting in higher toughness (which depicts both elastic and plastic deformations). To simply compare the role of fiber type, resin type, and stacking sequence on the LVI characteristics of various HTCLs investigated in this study, the LVI results at the impact energy level of 33 J (as an example) are summarized in Table 2.

Table 2. Impact maximum load, deflection, absorbed energy, and major damage energy for various HTCLs impacted at 33 J.

| Calculated properties | Maximum load (kN) | Maximum deflection (mm) | Absorbed energy (J) | Major damage energy (J) |
|---|---|---|---|---|
| HTCL-1E | 7.5 ± 0.2 | 5.6 ± 0.3 | 30.2 ± 0.8 | 0.47 ± 0.02 |
| HTCL-2E | 9.1 ± 0.3 | 6.8 ± 0.5 | 26.5 ± 0.6 | 18.5 ± 0.3 |
| HTCL-3E | 8.9 ± 0.4 | 5.8 ± 0.3 | 22.8 ± 0.5 | 23.5 ± 0.8 |
| HTCL-4E | 10.1 ± 0.3 | 6.2 ± 0.2 | 12.7 ± 0.3 | 30.5 ± 0.9 |
| HTCL-5E | 10.7 ± 0.6 | 5.4 ± 0.3 | 22.7 ± 0.7 | 23.5 ± 0.9 |
| HTCL-4P | 10.3 ± 0.2 | 5.8 ± 0.4 | 18.3 ± 0.4 | 31.0 ± 0.8 |

[1]E: Elium® resin, P: Epolam Resin

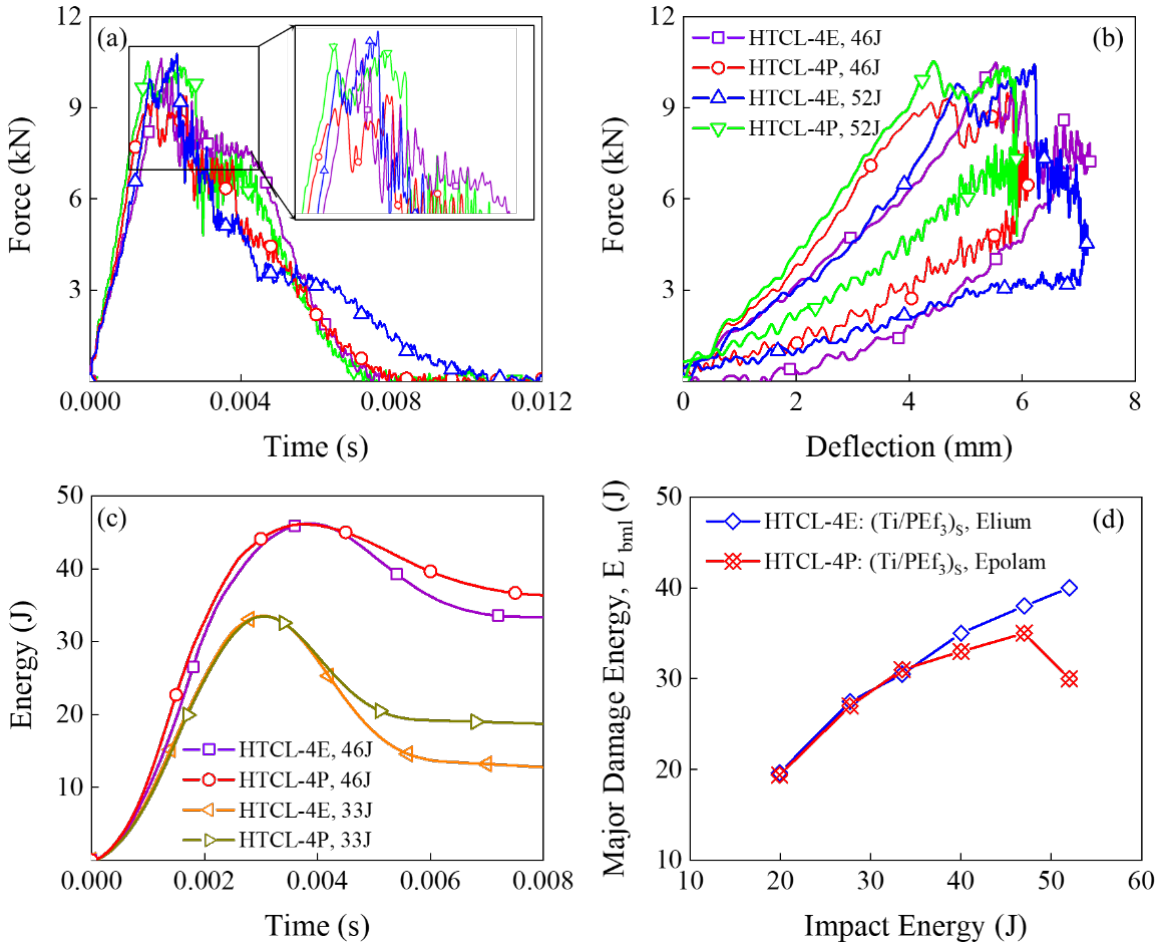


Fig. 12. Force-time (a), force-deflection (b), energy-time (c) and major damage energy (d) attributes of UHMWPE-based HTCLs with TP Elium® (HTCL-4E) and TS Epolam (HTCL-4P) subjected to different LVI tests

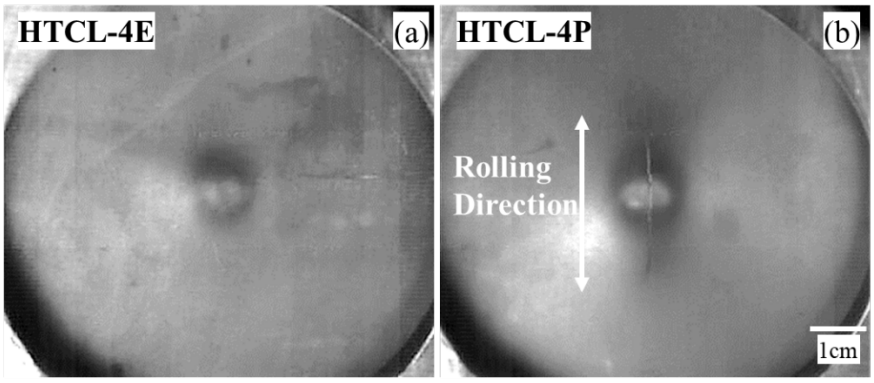


Fig. 13. The comparison of the non-impacted side images of Eium®-based Ti/UHMWPE (HTCL-4E) (a), and Epolam-based Ti/UHMWPE (HTCL-4P) (b) impacted at 40 J

# 4 Conclusion

The low-velocity impact (LVI) response of a new generation of thermoplastic (TP) hybrid titanium composite laminates (HTCLs) as high-performance light-weight fiber metal laminates (FMLs) was investigated. To do so, Ti-6Al-4V sheets, carbon fabrics, and ultra-high molecular weight polyethylene (UHMWPE) fabrics were used to fabricate multiple laminates with different fibers, metal volume fractions, and lamination layups. The resin infusion process at room temperature was used for developing the laminates with a novel liquid thermoplastic methyl methacrylate resin, Elium® 188. Prior to fabrication, a recently developed surface treatment was applied to the Ti alloy sheets to improve the bonding strength. In addition to TP-HTCLs, equivalent thermosetting (TS)-HTCLs with an epoxy resin, Epolam, were fabricated to compare the results and evaluate the possibility of Elium® resin to replace it with epoxy for industrial applications. Impact properties including contact force, displacement, energy parameters, and related damage modes were studied and presented. Regarding the LVI response of HTCLs, it is concluded that the HTCL with UHMWPE fabrics on the composite sides (before the Ti alloy sheets) performs better in LVI compared to that with brittle carbon fibers on the sides (of its composite core), since UHMWPE enjoys greater failure strain and toughness. As a result, the presence of the UHMWPE and Ti alloy at the sides makes the laminate more ductile. Furthermore, the new generation of TP-HTCL developed at room temperature shows enhanced out-of-plane performance compared to that of the TS counterpart. This promises further developments of TP-FMLs in general and TP-HTCLs in particular with improved impact behavior and reduced fabrication time and costs.

## Acknowledgments

The authors are grateful for the support from The Hong Kong University of Science and Technology (Grant #: R9365), the NSFC/HK Joint Research Scheme, (Grant#: N_HKUST 631/18), and Nanhai-HKUST Program (Grant #: FSNH-18FYTRI01), Guangzhou Municipal Science and Technology Bureau (Project #: 201907010024), and Science and Technological Bureau of Guangzhou Huangpu District (Project #: 2018GH04). The authors also would like to acknowledge Dr. Brian Dong and Dr. Jinchun Zhu of Arkema, Changshu Research and Development Center, China for providing Elium® resin.

## References

[1] Nakatani H, Kosaka T, Osaka K, Sawada Y. Damage characterization of titanium/GFRP hybrid laminates subjected to low-velocity impact. Composites Part A: Applied Science and Manufacturing. 2011;42(7):772-81.

[2] Vlot A, Gunnink JW. Fibre metal laminates: an introduction: Springer Science & Business Media; 2011.

[3] Morinière FD, Alderliesten RC, Sadighi M, Benedictus R. An integrated study on the low-velocity impact response of the GLARE fibre-metal laminate. Composite Structures. 2013;100:89-103.

[4] Yarmohammad Tooski M, Alderliesten RC, Ghajar R, Khalili SMR. Experimental investigation on distance effects in repeated low velocity impact on fiber–metal laminates. Composite Structures. 2013;99:31-40.

[5] Mottaghian F, Yaghoobi H, Taheri F. Numerical and experimental investigations into post-buckling responses of stainless steel- and magnesium-based 3D-fiber metal laminates reinforced by basalt and glass fabrics. Composites Part B: Engineering. 2020;200:108300.

[6] De Cicco D, Taheri F. Performances of magnesium- and steel-based 3D fiber-metal laminates under various loading conditions. Composite Structures. 2019;229:111390.

[7] Yaghoobi H, Mottaghian F, Taheri F. Enhancement of buckling response of stainless steel-based 3D-fiber metal laminates reinforced with graphene nanoplatelets: Experimental and numerical assessments. Thin-Walled Structures. 2021;165:107977.
[8] Chai GB, Manikandan P. Low velocity impact response of fibre-metal laminates – A review. Composite Structures. 2014;107:363-81.
[9] Sadighi M, Alderliesten RC, Benedictus R. Impact resistance of fiber-metal laminates: A review. International Journal of Impact Engineering. 2012;49:77-90.
[10] Li X, Zhang X, Zhang H, Yang J, Nia AB, Chai GB. Mechanical behaviors of Ti/CFRP/Ti laminates with different surface treatments of titanium sheets. Composite Structures. 2017;163:21-31.
[11] Asaee Z, Shadlou S, Taheri F. Low-velocity impact response of fiberglass/magnesium FMLs with a new 3D fiberglass fabric. Composite Structures. 2015;122:155-65.
[12] Alderliesten R, Rans C, Benedictus R. The applicability of magnesium based Fibre Metal Laminates in aerospace structures. Composites Science and Technology. 2008;68(14):2983-93.
[13] Kazemi ME, Shanmugam L, Yang L, Yang J. A review on the hybrid titanium composite laminates (HTCLs) with focuses on surface treatments, fabrications, and mechanical properties. Composites Part A: Applied Science and Manufacturing. 2020;128:105679.
[14] Fotouhi S, Clamp J, Bolouri A, Pozegic TR, Fotouhi M. Investigating polyethersulfone interleaved Glass/Carbon hybrid composite under impact and its comparison with GLARE. Composite Structures. 2019;226:111268.
[15] Bieniaś J, Jakubczak P, Droździel M, Surowska B. Interlaminar Shear Strength and Failure Analysis of Aluminium-Carbon Laminates with a Glass Fiber Interlayer after Moisture Absorption. Materials. 2020;13(13):2999.
[16] Li X, Zhang X, Guo Y, Shim VPW, Yang J, Chai GB. Influence of fiber type on the impact response of titanium-based fiber-metal laminates. International Journal of Impact Engineering. 2018;114:32-42.
[17] Reiner J, Torres JP, Veidt M, Heitzmann M. Experimental and numerical analysis of drop-weight low-velocity impact tests on hybrid titanium composite laminates. Journal of Composite Materials. 2016;50(26):3605-17.

[18] Bernhardt S, Ramulu M, Kobayashi AS. Low-Velocity Impact Response Characterization of a Hybrid Titanium Composite Laminate. Journal of Engineering Materials and Technology. 2006;129(2):220-6.
[19] Cortes P, Cantwell WJJocm. The impact properties of high-temperature fiber-metal laminates. 2007;41(5):613-32.
[20] Jakubczak P, Bieniaś J, Droździel M. The collation of impact behaviour of titanium/carbon, aluminum/carbon and conventional carbon fibres laminates. Thin-Walled Structures. 2020;155:106952.
[21] Jakubczak P. The impact behaviour of hybrid titanium glass laminates—Experimental and numerical approach. International Journal of Mechanical Sciences. 2019;159:58-73.
[22] Shanmugam L, Feng X, Yang J. Enhanced interphase between thermoplastic matrix and UHMWPE fiber sized with CNT-modified polydopamine coating. Composites Science and Technology. 2019;174:212-20.
[23] Ćwik TK, Iannucci L, Curtis P, Pope D. Investigation of the ballistic performance of ultra high molecular weight polyethylene composite panels. Composite Structures. 2016;149:197-212.
[24] Nazarian O, Zok FW. Shear-dominated plastic behavior of a cross-ply Dyneema® composite. Composites Part A: Applied Science and Manufacturing. 2014;67:316-23.
[25] O'Masta MR, Deshpande VS, Wadley HNG. Mechanisms of projectile penetration in Dyneema® encapsulated aluminum structures. International Journal of Impact Engineering. 2014;74:16-35.
[26] Kazemi ME, Shanmugam L, Lu D, Wang X, Wang B, Yang J. Mechanical properties and failure modes of hybrid fiber reinforced polymer composites with a novel liquid thermoplastic resin, Elium®. Composites Part A: Applied Science and Manufacturing. 2019;125:105523.
[27] Shanmugam L, Kazemi ME, Qiu C, Rui M, Yang L, Yang J. Influence of UHMWPE fiber and Ti6Al4V metal surface treatments on the low-velocity impact behavior of thermoplastic fiber metal laminates. Advanced Composites and Hybrid Materials. 2020;3(4):508-21.

[28] Mamalis D, Obande W, Koutsos V, Blackford JR, Ó Brádaigh CM, Ray D. Novel thermoplastic fibre-metal laminates manufactured by vacuum resin infusion: The effect of surface treatments on interfacial bonding. Materials & Design. 2019;162:331-44.
[29] Kazemi ME, Shanmugam L, Chen S, Yang L, Yang J. Novel thermoplastic fiber metal laminates manufactured with an innovative acrylic resin at room temperature. Composites Part A: Applied Science and Manufacturing. 2020;138:106043.
[30] Kazemi ME, Shanmugam L, Dadashi A, Shakouri M, Lu D, Du Z, et al. Investigating the roles of fiber, resin, and stacking sequence on the low-velocity impact response of novel hybrid thermoplastic composites. Composites Part B: Engineering. 2021;207:108554.
[31] Obande W, Ó Brádaigh CM, Ray D. Continuous fibre-reinforced thermoplastic acrylic-matrix composites prepared by liquid resin infusion – A review. Composites Part B: Engineering. 2021;215:108771.
[32] Obande W, Ó Brádaigh CM, Ray D. Thermoplastic hybrid-matrix composite prepared by a room-temperature vacuum infusion and in-situ polymerisation process. Composites Communications. 2020;22:100439.
[33] Bhudolia SK, Joshi SC, Bert A, Gohel GR, Raama M. Energy Characteristics and Failure Mechanisms for Textile Spread Tow Thin Ply Thermoplastic Composites under Low-velocity Impact. Fibers and Polymers. 2019;20(8):1716-25.
[34] Bhudolia SK, Gohel G, Kantipudi J, Leong KF, Barsotti RJ. Ultrasonic Welding of Novel Carbon/Elium® Thermoplastic Composites with Flat and Integrated Energy Directors: Lap Shear Characterisation and Fractographic Investigation. Materials. 2020;13(7):1634.
[35] Shanmugam L, Kazemi M, Yang J. Improved bonding strength between thermoplastic resin and Ti alloy with surface treatments by multi-step anodization and single-step microarc oxidation method: a comparative study. ES Materials & Manufacturing. 2019;3:57-65.
[36] Shanmugam L, Kazemi ME, Yang J. Improved Bonding Strength Between Thermoplastic Resin and Ti Alloy with Surface Treatments by Multi-step Anodization and Single-step Micro-arc Oxidation Method: A Comparative Study. ES Materials & Manufacturing. 2019;3:57-65.
[37] Batra RC, Gopinath G, Zheng JQ. Damage and failure in low energy impact of fiber-reinforced polymeric composite laminates. Composite Structures. 2012;94(2):540-7.

[38] Körbelin J, Derra M, Fiedler B. Influence of temperature and impact energy on low velocity impact damage severity in CFRP. Composites Part A: Applied Science and Manufacturing. 2018;115:76-87.
[39] Bhudolia SK, Kam KK, Perrotey P, Joshi SC. Effect of fixation stitches on out-of-plane response of textile non-crimp fabric composites. Journal of Industrial Textiles. 2019;48(7):1151-66.
[40] Bhudolia SK, Joshi SC. Low-velocity impact response of carbon fibre composites with novel liquid Methylmethacrylate thermoplastic matrix. Composite Structures. 2018;203:696-708.
[41] Kinvi-Dossou G, Matadi Boumbimba R, Bonfoh N, Koutsawa Y, Eccli D, Gerard P. A numerical homogenization of E-glass/acrylic woven composite laminates: Application to low velocity impact. Composite Structures. 2018;200:540-54.
[42] Shanmugam L, Kazemi ME, Li Z, Luo W, Xiang Y, Yang L, et al. Low-velocity impact behavior of UHMWPE fabric/thermoplastic laminates with combined surface treatments of polydopamine and functionalized carbon nanotubes. Composites Communications. 2020;22:100527.
[43] Fotouhi M, Damghani M, Leong MC, Fotouhi S, Jalalvand M, Wisnom MR. A comparative study on glass and carbon fibre reinforced laminated composites in scaled quasi-static indentation tests. Composite Structures. 2020;245:112327.
[44] Caprino G, Lopresto V, Scarponi C, Briotti G. Influence of material thickness on the response of carbon-fabric/epoxy panels to low velocity impact. Composites Science and Technology. 1999;59(15):2279-86.
[45] Abrate S. Impact engineering of composite structures: Springer Science & Business Media; 2011.